13. Regenfus, C. A cryogenic silicon micro strip and pure-CsI detector for detection of antihydrogen annihilations. *Nucl. Instrum. Methods A* (in the press).
14. Bendiscioli, G. & Kharzeev, D. Antinucleon–nucleon and antinucleon–nucleus interaction, a review of experimental data. *Rivista Nuovo. Cim.* **17(6),** 1–42 (1994).
15. Amsler, C. *et al.* Temperature dependence of pure CsI: scintillation light yield and decay time. *Nucl. Instrum. Methods A* **480,** 494–500 (2002).
16. Charlton, M. & Humberston, J. W. *Positron Physics* (Cambridge Univ. Press, Cambridge, 2001).
17. Gabrielse, G. *et al.* First positron cooling of antiprotons. *Phys. Lett. B* **507,** 1–6 (2001).
18. Calligarich, E., Dolfini, R., Genoni, M. & Rotondi, A. A fast algorithm for vertex estimation. *Nucl. Instrum. Methods A* **311,** 151–155 (1992).

Acknowledgements

The authors comprise the ATHENA Collaboration. We would like to thank G. Bendiscioli, S. Bricola, P. Chiggiato, J. Hansen, H. Higaki, A. Lanza, C. Marciano, O. Meshkov, P. Salvini, G. Sobrero, B. Schmid and E. Søndergaard. We also thank the CERN AD team and C. Surko, who provided essential advice. This work was supported by Istituto Nazionale di Fisica Nucleare (Italy), Conselho Nacional de Desenvolvimento Científico e Technológico, Fundação de Amparo a Pesquisa do Estado do Rio de Janeiro (FAPERJ) e Fundação CCMN/UFRJ (Brazil), Grant-in-Aid for Creative Basic Research of Monbukagakusho (Japan), the Swiss National Science Foundation, the Danish Natural Science Research Council, The UK Engineering and Physical Sciences Research Council (EPSRC), The EU (Eurotraps Network), and the Royal Society. L.V.J., M.H.H., M.C. and J.S.H. acknowledge the work of the late B. Deutch.

Competing interests statement

The authors declare that they have no competing financial interests.

Correspondence and requests for material should be addressed to J.S.H. (e-mail: jeffrey.hangst@cern.ch).

Quantum phase transition in a common metal

A. Yeh*†, Yeong-Ah Soh*, J. Brooke*†, G. Aeppli*, T. F. Rosenbaum† & S. M. Hayden‡

* *NEC Research Institute, 4 Independence Way, Princeton, New Jersey 08540, USA*
† *The James Franck Institute and Department of Physics, The University of Chicago, Illinois 60637, USA*
‡ *H.H. Wills Physics Laboratory, University of Bristol, Bristol BS8 1TL, UK*

The classical theory of solids, based on the quantum mechanics of single electrons moving in periodic potentials, provides an excellent description of substances ranging from semiconducting silicon to superconducting aluminium. Over the last fifteen years, it has become increasingly clear that there are substances for which the conventional approach fails. Among these are certain rare earth compounds[1,2] and transition metal oxides[3,4], including high-temperature superconductors[5,6]. A common feature of these materials is complexity, in the sense that they have relatively large unit cells containing heterogeneous mixtures of atoms. Although many explanations have been put forward for their anomalous properties[7], it is still possible that the classical theory might suffice. Here we show that a very common chromium alloy has some of the same peculiarities as the more exotic materials, including a quantum critical point[8], a strongly temperature-dependent Hall resistance[4,5] and evidence for a 'pseudogap'[9]. This implies that complexity is not a prerequisite for unconventional behaviour. Moreover, it should simplify the general task of explaining anomalous properties because chromium is a relatively simple system in which to work out in quantitative detail the consequences of the conventional theory of solids.

Apart from complexity, a feature shared by almost all metals whose properties are at odds with conventional theory is proximity to magnetic instabilities[10,11], that is, the materials are nearly magnetic, and when placed under pressure or their chemical formulae are slightly changed, they acquire magnetic order. A unique point in the associated pressure (or composition)–temperature phase diagrams is where the ordering temperatures vanish. Quantum rather than thermal fluctuations destroy the order beyond this point, which is therefore referred to as 'quantum critical'.

We have selected chromium for our experiment because it is the simplest metal close to a quantum critical point. Indeed, it is a body-centred cubic (b.c.c.) antiferromagnet, whose magnetism[12] can be made to disappear with modest substitution of vanadium, its neighbour in the periodic table. On increasing the vanadium concentration x from 0, the Néel temperature T_N (Fig. 1a) and ordered magnetic moment[13] (Fig. 1b) for $Cr_{1-x}V_x$ vanish continuously at the quantum critical point with $x_c = 0.035$. There is a wealth of information[14] on this and other alloys of Cr, but, remarkably for such a simple substance, basic quantities such as the Hall resistance, which have engendered so much excitement for other materials from semiconductor heterostructures to high-temperature superconductors[5], have not been studied systematically. The Hall effect has until now received little attention in the context of quantum phase transitions, and to our knowledge, our experiments are the first to examine the variation of the Hall effect near an antiferromagnetic quantum phase transition in Cr (ref. 15) or in any metal.

Our experiments were performed on single crystals, and the details are in the legend of Fig. 2. We plot in Fig. 2a the longitudinal resistivity $\rho(T)$ for several samples on each side of x_c. A key feature[12,15] is the "chromium anomaly" at T_N, where the resistivity increases owing to a loss of the carriers localized through magnetic ordering. The anomaly rides on a background that consists of a composition-dependent constant and a T-dependent term. The former grows primarily with the disorder, which increases with increased (random) alloying, although there is a small anomaly at x_c (ref. 16). The latter does not vary significantly with composition, and, as demonstrated in the inset to Fig. 2a, appears to follow a

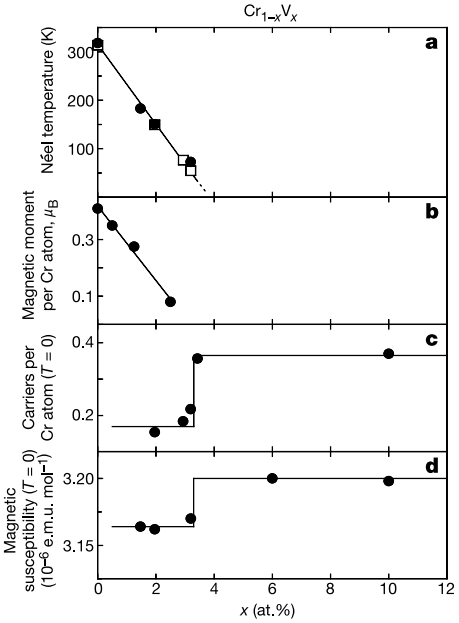

Figure 1 Magnetic ordering (Néel) temperature and zero-temperature properties of $Cr_{1-x}V_x$ near its quantum critical point. **a**, Phase diagram for the isostructural dilution series $Cr_{1-x}V_x$, where the filled circles and open squares denote Néel temperatures obtained from magnetic susceptibility and Hall effect data, respectively. **b**, Ordered magnetic moment measured by magnetic neutron diffraction[13] at 4.2 K for $Cr_{1-x}V_x$. **c**, Low-temperature ($T < 5$ K) carrier density obtained from inverse of the Hall number. **d**, Low-temperature magnetic susceptibility.

simple T^3 power law at low T for all x. This is in sharp contrast to the rare-earth compound $Ce(Cu,Au)_6$ which has the most thoroughly studied[1,2] quantum critical point among metals and shows $\rho(T)$ changing from T^2 a power-law to T and then back to T^2 again when passing through x_c. It also differs from various transition metal oxides where magnetic field or composition tuning achieves results[6,17] similar to those for $CeCu_6$. Furthermore, even the quadratic law $\rho(T) \propto T^2$, characteristic of conventional interacting Fermi liquids, is not detectable in $Cr_{1-x}V_x$ data. However, our experimental result agrees with one of the main predictions of the theory of antiferromagnetic quantum critical points in metals[18,19]: the temperature dependence of the longitudinal resistivity remains indifferent to x.

The Hall effect, where the deflection of the carriers in a magnetic field gives rise to a voltage perpendicular to the current and field directions, turns out to be far more sensitive to the quantum critical point. We plot in Fig. 2b the measured inverse Hall numbers, expressed as carrier densities, as a function of T for a variety of V concentrations. The spin-density-wave transition has a proportionately much larger effect on $1/R_H(T)$ than on $\rho(T)$; Fermi surface destruction manifests itself immediately as a change in the Hall number. The Hall number at low T increases by 100% in a narrow interval about x_c, jumping from one value weakly dependent on x for $x < x_c$ to an x-independent value for $x > x_c$ (Fig. 1c). The $T = 0$ phase transition seems to involve the destruction of a fixed amount of Fermi surface, and the quantum critical point simply occurs when this destruction is no longer possible. Even more remarkable is the strong temperature dependence of $1/R_H$ above $T_N(x)$, which is on the same scale as that which has attracted so much attention in the case of exotic metals such as the cuprates[5]. In the simplest interpretation, this effect implies an ever-increasing loss of carriers above the Néel temperature as x_c is approached from above.

The exceptional temperature dependence of the Hall coefficient in the high-temperature superconductors is accompanied by different temperature dependencies for the longitudinal and transverse conductivities[5]. We find similar behaviour for $Cr_{1-x}V_x$. We plot in Fig. 3a the ratio $\cot\theta_H$ of transverse to longitudinal conductivities at $H = 1.5$ T. The approximately T^2 dependence contrasts with the T^3 behaviour of the longitudinal resistivity (Fig. 2a), and is consistent with similar temperature dependencies seen not only for the high-temperature superconductors but also for $V_{2-y}O_3$ (ref. 4).

The Hall effect can be difficult to interpret because for multiple bands crossing the Fermi energy E_F, it depends on carrier mobilities as well as densities[20], making it useful to examine another quantity sensitive to the carrier density at E_F. We have chosen to measure the bulk magnetic susceptibility χ, which for simple metals is proportional to the density of states at the Fermi level. Because of problems with surface oxides (see inset of Fig. 3b), measurements of

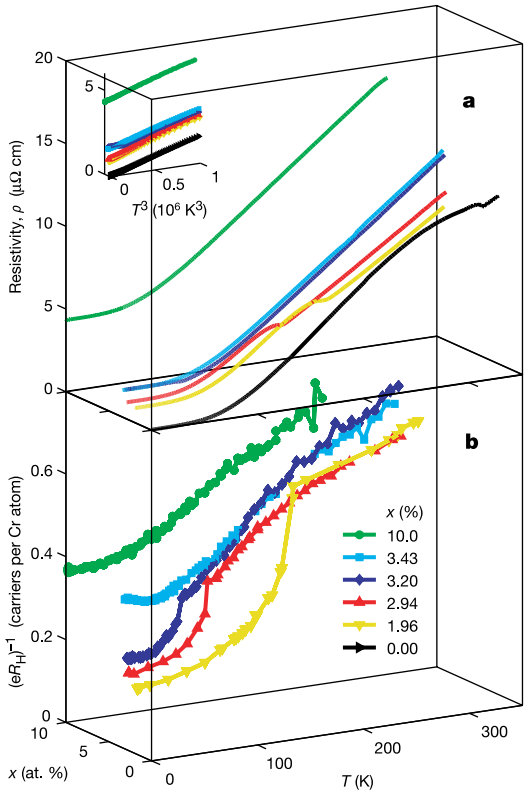

Figure 2 Temperature-dependent electrical properties near the quantum critical point of $Cr_{1-x}V_x$. Resistivity (**a**) and inverse Hall number (**b**) versus temperature T for various $Cr_{1-x}V_x$ samples. Inset in **a** displays the resistivity as a function of T^3. Although the carrier density jumps at x_c, the T-dependent resistivity continues smoothly through the quantum critical point. The Hall number is positive for Cr and its alloys[15], implying that holes are more important contributors than electrons. The samples used in our experiments are single crystals of $Cr_{1-x}V_x$ grown by Ames Laboratory in an arc zone refining furnace, usually from 99.995% pure Cr and 99.9% pure V and annealed for 72 h at 1,600 °C to relieve internal strain. Laué backscattering was used to determine the orientation of the b.c.c. lattice, and several pieces aligned with the (100) crystallographic direction were cut from the centre of each crystal using spark erosion. Proper etching to remove the surface oxide (with a 3:1::HCl:H_2O_2 solution quenched with THF) is essential for reproducible results. Increased temperatures (30 to 60 °C) and an ultrasonic bath were used to speed the etching process. For the resistivity and Hall measurements, the samples were parallelepipeds and small gold pads (~1,000 Å thick) were evaporated onto opposite sides of the parallelepipeds for use as electrical contacts. Indium solder and 1-mm-diameter gold wires connected the gold pads to the measurement circuit. The absolute value of the low-temperature (T) resistivity (~1 μΩ cm) indicates that the crystals are in the 'clean' limit, where disorder is unlikely to play a significant role. The magnetotransport measurements were performed in a top-loading ^{3}He system using standard low-frequency lock-in methods.

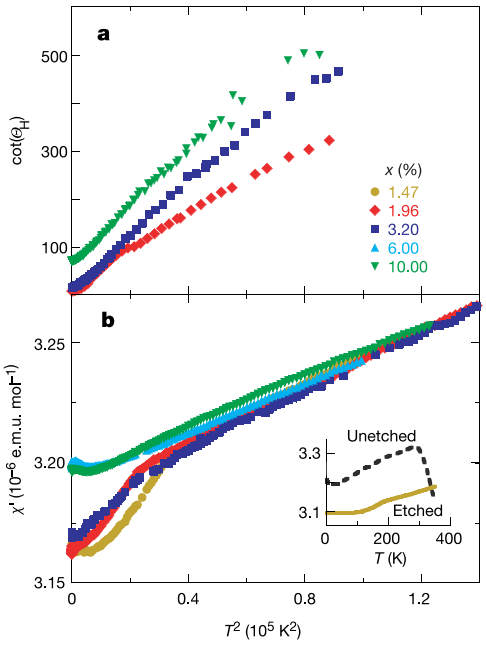

Figure 3 Electronic scattering and density of states, as measured by temperature dependence of electrical conductivity and magnetic susceptibility. **a**, Cotangent of Hall angle $\cot(\theta_H) = \sigma_{xx}/\sigma_{xy} = \rho/(HR_H)$, where σ is electrical conductivity and the field H is fixed at 1.5 T. **b**, Magnetic susceptibility χ' as a function of T^2 for various $Cr_{1-x}V_x$ samples. The data for χ' were all collected in fields of 3.2 and 3.6 T and cross-normalized to yield the same value above 370 K. Inset in **b** shows the importance of proper etch treatment of samples: the $x = 0.0147$ crystal used here does not reveal its intrinsic antiferromagnetic transition at 180 K unless the etch is performed.

the magnetic susceptibility of Cr and its alloys are rare, and if available, contradictory[14]. We have therefore collected our own data using a Quantum Design SQUID (superconducting quantum interference device) magnetometer. For ordinary insulating antiferromagnets, reducing T leads to a χ increasing towards a maximum at T_N, below which it decreases again. Chromium and its alloys behave quite differently (Fig. 3b): χ decreases in proportion to T^2 down to T_N, below which there is a sharp downturn which mirrors the behaviour of the inverse Hall coefficient (Fig. 2b). Here too, samples with $x < x_c$ and $x > x_c$ segregate into two classes (Fig. 1d), separated by a sharp change in the $T \rightarrow 0$ value of the susceptibility.

What is the origin of the increases of $1/R_H$ and χ with T in the paramagnetic regime on both sides of the quantum critical point? Ordinary band theory clearly yields the observed reduction of $1/R_H$ and χ on entering the ordered state for $x < x_c$, through a reduction in the density of states at the Fermi level arising because of the destruction of parts of the Fermi surface. Band theory can also account for increases of χ and $1/R_H$ with T in the paramagnetic regime with $T > T_N(x)$, provided that the Fermi energy lies at a minimum in the electronic density of states: warming would increase the density of states sampled. It is certainly possible for the minimum to be close to the Fermi energy, as has been computed for magnetically ordered Cr (ref. 21), although there are also calculations[22] that show this not to be the case for paramagnetic Cr. Another prediction of band theory, which gives relatively small band masses for $Cr_{1-x}V_x$, is that as the content of V—with its outer electron count different from that of Cr—is varied, the Fermi level would shift significantly away from the minimum, flattening the T-dependence of $\chi(T)$ and $1/R_H(T)$ over the temperature ranges which we have examined. This is clearly not what we see in our data, which, in the paramagnetic phase, vary little with x, suggesting a minimum pinned at the Fermi level independently of band filling as regulated by V content.

The apparent failure of band theory in dealing with our transport data is also consistent with its failure (by a factor of 28) to account for the antiferromagnetic spin fluctuations[23,24] in $Cr_{0.95}V_{0.05}$. This leaves us with the following facts to aid the search for an explanation of a minimum tied to the Fermi level: (1) $1/R_H$ decreases with T both in the paramagnetic phase, above $T_N(x)$, as well as upon entering the Néel state, below $T_N(x)$. As x increases towards x_c, the reduction in $1/R_H$ below T_N is diminished, while the amount by which $1/R_H$ decreases between 400 K and T_N is correspondingly increased. Taking $1/R_H$ as a measure of the effective Fermi surface area, there seems to be a trade-off between Fermi surface 'lost' below and above $T_N(x)$—apparently the magnetic fluctuations found above $T_N(x)$ can be as powerful in diminishing the Fermi surface as is the magnetic order below $T_N(x)$. (2) An ordered spin-density wave induces a gap in the density of states for the Fermi surfaces involved. The gap is visible in optical data for Cr (ref. 25). (3) There are strong[24] antiferromagnetic fluctuations extending to very high energy (>0.4 eV) for paramagnetic $Cr_{1-x}V_x$. The fluctuations are patches of material with short-lived order of the type stabilized for infinite times and distances in the ordered phase.

Putting facts (1) to (3) together makes a pseudogap derived from the antiferromagnetic fluctuations the most probable cause of the minimum in the density of states seemingly pinned at the Fermi level. The idea is that over the lifetime of the antiferromagnetic critical fluctuations, a gap like that seen in the ordered phase (point (2)) will develop[26]. Because the lifetime is not truly infinite at any finite temperature, we will see a smoothed and somewhat filled gap, or 'pseudogap', akin to what has caused so much excitement in the study of the copper oxides[9]. A direct measurement of the density of states, such as the magnetic susceptibility, will be sensitive to this pseudogap, as will transport properties involving timescales of the order of, or shorter than, the lifetime of the critical fluctuations. Both Figs 2b and 3b indicate that the pseudogap is felt deep into the paramagnet: a substantive variation in $1/R_H(T)$ and $\chi(T)$ remains for V doping as high as 10%, three times x_c. That the variation is related to the magnetism of the undoped parent, rather than the consequence of conventional multiband effects, follows from point (1)—the variation induced by Néel order can be traded against that seen above $T_N(x)$. Furthermore, for $x = 0.05$, the inverse lifetime of the critical fluctuations is 0.1 eV (ref. 24), well below the width of the conduction band from which the carriers responsible for both metallicity and magnetism are drawn. This means that they live long enough to affect transport properties. Most notably, such fluctuations will tie down electrons from within the Fermi surface in the same way that magnetic order ties down electrons, implying an apparent loss of carriers on cooling as the fluctuations slow down. We conclude that in this common transition metal, we are finding pseudogap behaviour and a localization of charge, as evidenced by a highly temperature-dependent Hall effect, of the type hitherto associated only with exotic multicomponent materials such as the transition metal oxides.

We have performed the first measurements of the Hall effect—the simplest macroscopic probe of Fermi surface integrity—near a quantum critical point where metallic antiferromagnetism vanishes. The quantum critical point does not occur in a complex substance, but instead in a simple alloy whose properties should be calculable using a modern computer and the band theory of solids, thus providing an unusually rigorous baseline for finding unconventional behaviour. One aim of this paper is to encourage such computations of the Hall effect.

Our experiments yield two important results. The first, discussed in the previous paragraph, is that the T-dependent Hall effect is reminiscent of that for much more exotic metals, and, together with susceptibility data, implies a pseudogap in the spectrum of electronic excitations. The second is that the Hall effect evolves rather more quickly near the quantum phase transition than the magnetic order. Figure 1, which provides a summary of current knowledge about the quantum critical point in $Cr_{1-x}V_x$, puts the $T = 0$ charge and spin properties into perspective. The Hall effect (Fig. 1c), as well as our magnetic susceptibility data (Fig. 1d) indicate that as far as the Fermi surfaces are concerned, the $T = 0$ quantum phase transition is an either/or proposition. What this means is that as we scan vanadium composition x, we either see (for $x < x_c$) magnetic order involving a fixed number of carriers and a particular Fermi surface or (for $x > x_c$) disorder involving a different fixed number and another, larger Fermi surface. This quality contrasts with conventional expectations[27,28] and the behaviour (Fig. 1b) of the order parameter itself, which vanishes more gradually as the quantum critical point is approached. Thus, near the quantum critical point, there are large amplitude fluctuations in the Fermi surface area, and these are likely to be connected to the anomalous finite temperature properties of $Cr_{1-x}V_x$, as has also been concluded[2] for the quantum critical point in $Ce(Cu,Au)_6$. □

Received 17 July; accepted 5 August 2002; doi:10.1038/nature01044.

1. Löhneysen, H. v. *et al.* Non-Fermi-liquid behavior in a heavy-fermion alloy at a magnetic instability. *Phys. Rev. Lett.* **72,** 3262–3265 (1994).
2. Schröder, A. *et al.* Onset of antiferromagnetism in heavy-fermion metals. *Nature* **407,** 351–355 (2000).
3. Varma, C. M. *et al.* Phenomenology of the normal state of Cu-O high temperature superconductors. *Phys. Rev. Lett.* **63,** 1996–1999 (1989).
4. Rosenbaum, T. F., Husmann, A., Carter, S. A. & Honig, J. M. Temperature dependence of the Hall angle in a correlated three-dimensional metal. *Phys. Rev. B* **57,** R13997–R13999 (1998).
5. Chien, T. R., Brawner, D. A., Wang, Z. Z. & Ong, N. P. Unusual $1/T^3$ temperature dependence of the Hall conductivity in $YBa_2Cu_3O_{7-\delta}$. *Phys. Rev. B* **43,** 6242–6245 (1991).
6. Grigera, S. A. *et al.* Magnetic field-tuned quantum criticality in the metallic ruthenate $Sr_3Ru_2O_7$. *Science* **294,** 329–332 (2001).
7. Allen, P. B. Superconductivity: Is kinky conventional? *Nature* **412,** 494–495 (2001).
8. Sachdev, S. *Quantum Phase Transitions* (Cambridge Univ. Press, Cambridge, 1999).
9. Timusk, T. & Statt, B. The pseudogap in high-temperature superconductors: an experimental overview. *Rep. Prog. Phys.* **62,** 61–122 (1999).
10. Aeppli, G., Mason, T. E., Hayden, S. M., Mook, H. A. & Kulda, J. Nearly singular magnetic fluctuations in the normal state of a high-T_c cuprate superconductor. *Science* **278,** 1432–1435 (1997).
11. Aeppli, G. & Broholm, C. *Handbook of the Physics and Chemistry of the Rare Earths* Vol. 19 123–175 (Elsevier, Amsterdam, 1994).

12. Fawcett, E. Spin-density-wave antiferromagnetism in chromium. *Rev. Mod. Phys.* **60,** 209–283 (1988).
13. Koehler, W. C., Moon, R. M., Trego, A. I. & Mackintosh, A. R. Antiferromagnetism in Chromium Alloys. I. Neutron Diffraction. *Phys. Rev.* **151,** 405–413 (1966).
14. Fawcett, E., Alberts, H. V., Galkin, V. Yu., Noakes, D. R. & Yakhmi, J. V. Spin-density wave antiferromagnetism in chromium alloys. *Rev. Mod. Phys.* **66,** 25–127 (1994).
15. de Vries, G. The transition in chromium and in some alloys of chromium with small amounts of other transition elements. *J. Phys. Rad.* **20,** 438–439 (1959).
16. Takeuchi, J., Sasakura, H. & Masuda, Y. Spin fluctuations in itinerant electron antiferromagnetic $Cr_{1-x}V_x$ system. *J. Phys. Soc. Jpn* **49,** 508–513 (1980).
17. Takagi, H. *et al.* Systematic evolution of temperature-dependent resistivity in $La_{2-x}Sr_xCuO_4$. *Phys. Rev. Lett.* **69,** 2975–2978 (1992).
18. Millis, A. J. Effect of a nonzero temperature on quantum critical points in itinerant fermion systems. *Phys. Rev. B* **48,** 7183–7196 (1993).
19. Hlubina, R. & Rice, T. M. Resistivity as a function of temperature for models with hot spots on the Fermi surface. *Phys. Rev. B* **52,** 9253–9260 (1995).
20. Furuya, Y. Temperature and magnetic field dependence of the Hall coefficient on the antiferromagnetic chromium. *J. Phys. Soc. Jpn* **40,** 490–497 (1976).
21. Hirai, K. Electronic structure of sinusoidal spin density wave state in chromium. *J. Phys. Soc. Jpn* **62,** 690–703 (1993).
22. Laurent, D. G., Callaway, J., Fry, J. L. & Brener, N. E. Band structure, Fermi surface, Compton profile, and optical conductivity of paramagnetic chromium. *Phys. Rev. B* **23,** 4977–4987 (1981).
23. Staunton, J. B., Poulter, K., Ginatempo, B., Bruno, E. & Johnson, D. D. Incommensurate and commensurate antiferromagnetic spin fluctuations in Cr and Cr alloys from *ab initio* dynamical spin susceptibility calculations. *Phys. Rev. Lett.* **82,** 3340–3343 (1999).
24. Hayden, S. M., Doubble, R., Aeppli, G., Perring, T. G. & Fawcett, E. The strongly enhanced magnetic excitations near the quantum critical point of $Cr_{1-x}V_x$ and why strong exchange enhancement need not imply heavy fermion behavior. *Phys. Rev. Lett.* **84,** 999–1003 (2000).
25. Basov, D. N., Singley, E. J. & Dordevic, S. V. Sum rules and electrodynamics of high-T_c cuprates in the pseudogap state. *Phys. Rev. B* **65,** 054516 (2002).
26. Rosch, A. Some remarks on pseudogap behavior of nearly antiferromagnetic metals. *Phys. Rev. B* **64,** 174407 (2001).
27. Coleman, P., Pepin, C., Si, Q. & Ramazashvili, R. How do Fermi liquids get heavy and die? *J. Phys. Cond. Mat.* **13,** R723–R738 (2001).
28. Si, Q., Rabello, S., Ingersent, K. & Lleweilun Smith, J. Locally critical quantum phase transitions in strongly correlated metals. *Nature* **413,** 804–808 (2001).

Acknowledgements

We are grateful to P. Coleman and Q. Si for discussions. The work at the University of Chicago was supported by the National Science Foundation.

Competing interests statement

The authors declare that they have no competing financial interests.

Correspondence and requests for materials should be addressed to G.A. (e-mail: gabe@research.nj.nec.com).

Light-induced conversion of an insulating refractory oxide into a persistent electronic conductor

Katsuro Hayashi*, Satoru Matsuishi*†, Toshio Kamiya*†, Masahiro Hirano* & Hideo Hosono*†

** Transparent Electro-Active Materials Project, Exploratory Research for Advanced Technology (ERATO), Japan Science and Technology Corporation, KSP C-1232, 3-2-1 Sakado, Tatatsu-ku, Kawasaki 213-0012, Japan*
† Materials and Structures Laboratory, Tokyo Institute of Technology, Nagatsuta, Midori-ku, Yokohama 226-8503, Japan

Materials that are good electrical conductors are not in general optically transparent, yet a combination of high conductivity and transparency is desirable for many emerging opto-electronic applications[1–6]. To this end, various transparent oxides composed of transition or post-transition metals (such as indium tin oxide) are rendered electrically conducting by ion doping[1–6]. But such an approach does not work for the abundant transparent oxides of the main-group metals. Here we demonstrate a process by which the transparent insulating oxide $12CaO{\cdot}7Al_2O_3$ (refs 7–13) can be converted into an electrical conductor. H^- ions are incorporated into the subnanometre-sized cages of the oxide by a thermal treatment in a hydrogen atmosphere; subsequent irradiation of the material with ultraviolet light results in a conductive state that persists after irradiation ceases. The photo-activated material exhibits moderate electrical conductivity ($\sim$0.3 S cm^{-1}) at room temperature, with visible light absorption losses of only one per cent for 200-nm-thick films. We suggest that this concept can be applied to other main-group metal oxides, for the direct optical writing of conducting wires in insulating transparent media and the formation of a high-density optical memory.

The crystal lattice of $12CaO{\cdot}7Al_2O_3$ (refs 7–13) (C12A7) belongs to the space group of $I\bar{4}3d$ with a lattice constant of 1.199 nm (ref. 7), and the unit cell includes two molecules and twelve cages having a free space of $\sim$0.4 nm in diameter (Fig. 1a). The chemical formula for the unit cell may be represented as $[Ca_{24}Al_{28}O_{64}]^{4+} + 2O^{2-}$: the former denotes the lattice framework and the latter are called 'free oxygen ions'. Thus each cage has a mean effective charge of +1/3 (+4 charge/12 cages), leading to the expectation that such a positively charged cage behaves like an F^+ centre[14–17] upon capturing an electron. Another unique feature is the presence of the 'free oxygen ion', where an O^{2-} anion is accommodated in a cage to compensate for the positively charged framework[7,8] and is coordinated with six Ca^{2+} cations that constitute a part of the cage wall. The inter-ionic spacing between the free oxygen ion and the Ca^{2+} cation is about 1.5 times longer than the sum (0.24 nm) of their ionic radii, indicating that the free oxygen ion is loosely bound in the cage. The cage has 'entrances' which are about 0.1 nm in diameter, and they may control mass transport between the inner cages and the outside. These features provide flexibility for replacing

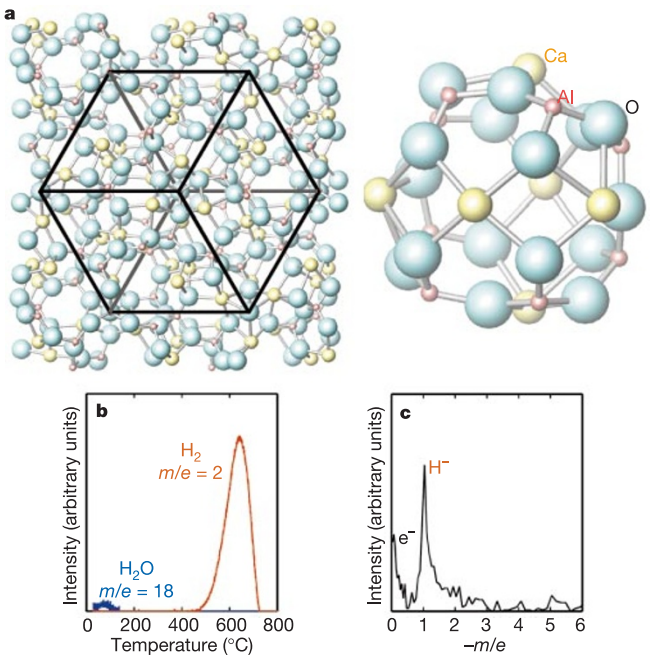

Figure 1 Incorporation of H^- ions in C12A7. **a**, Left is the crystal structure of C12A7 viewed from a ⟨111⟩ direction. A unit cell (lattice constant of 1.199 nm) with $Z = 2$ is indicated by a black frame. Right is the structure of a cage. Six Ca^{2+} ions coordinate to the centre of the cage. **b**, Thermogravimetric-mass spectroscopy (TG-MS) analysis on C12A7:H. Polycrystalline C12A7:H was heated at a rate of 10 K min^{-1} in a He atmosphere. Intense signal at $m/e = 2$ around 700 °C is attributed to the H_2 molecule. **c**, Time-of-flight mass spectrum of field-extracted ions from polycrystalline C12A7:H. Extraction field is 300 V cm^{-1}. Sample temperature is 710 °C. Two peaks at $-m/e = 0$ and 1 correspond to an electron and H^-, respectively.